**Manh Hoc Ha**
Ho Chi Minh City University of Technology (HCMUT)
Vietnam National University Ho Chi Minh City (VNU-HCM)
Vietnam

**Binh Thanh Tran**
Ho Chi Minh City University of Technology (HCMUT)
Vietnam National University Ho Chi Minh City (VNU-HCM)
Vietnam

**Nguyen Khanh Le**
Ho Chi Minh City University of Technology (HCMUT)
Vietnam National University Ho Chi Minh City (VNU-HCM)
Vietnam

**Minh Quang Pham**
Ho Chi Minh City University of Technology (HCMUT)
Vietnam National University Ho Chi Minh City (VNU-HCM)
Vietnam

**Quan Thien Phan Nghiem**
Ho Chi Minh City University of Technology (HCMUT)
Vietnam National University Ho Chi Minh City (VNU-HCM)
Vietnam

**Thong Duc Hong**
Ho Chi Minh City University of Technology (HCMUT)
Vietnam National University Ho Chi Minh City (VNU-HCM)
Vietnam

# Numerical Analysis Performance, Combustion, and Emissions of a Stationary Diesel Engine Operating on Ammonia-diesel Blends

*Ammonia is gaining attention as a promising alternative fuel due to its carbon-free composition and potential to reduce harmful emissions. This study investigates the effect of ammonia, used as a dual fuel with diesel at ammonia energy concentrations of 10% or less, on the combustion, performance, and emissions of a stationary single cylinder compression ignition engine, utilizing the AVL BOOST simulation model. The RV-125 engine, a popular model for rural areas in Vietnam, is designed to operate within a speed range of 900 to 2400 rpm at 85% engine load, with three different combustion durations: 80, 100, and 120 crank angle degrees (CD80, CD100, and CD120). The results show that increasing the ammonia content to 10% of the fuel energy slightly improves engine power by approximately 1%, but it also leads to higher brake specific fuel consumption due to ammonia's lower energy density. When ammonia is present in the blend, the peaks of heat release rate (HRR) and in-cylinder pressure increase slightly at CD80 but decrease modestly at CD100 and CD120; meanwhile, the in-cylinder temperature peak is found to decrease gradually with longer CD values, and the timings of HRR, in-cylinder pressure, and temperature peaks are slightly retarded. The findings also show that blending ammonia significantly reduces NO□ emissions by more than 22% and CO emissions by approximately 27%, while soot emissions remain virtually unchanged. The study concludes that ammonia blending represents a promising alternative for mitigating harmful pollutants and greenhouse gas emissions without compromising engine power or efficiency. This work provides a crucial foundation for future research aimed at applying ammonia fuel for rural development in Vietnam.*

***Keywords:*** *ammonia, dual-fuel engine, combustion, performance, emissions, AVL BOOST.*

## 1. INTRODUCTION

Nowadays, the decline in fossil fuel reserves has emerged as a significant concern, driving technological innovations in engines and promoting the investigation of alternative fuel solutions to meet global energy demands [1,2]. In response to global environmental challenges such as the greenhouse effect, the International Maritime Organization convened its 80th Marine Environmental Protection Committee meeting to reach net-zero greenhouse gas (GHG) emissions from international shipping by 2050 [3]. To mitigate global warming, sectors such as manufacturing, shipping, and the automotive industries must undergo comprehensive decarbonization. In this regard, the development and utilization of low-carbon and carbon-neutral alternative fuels, including Pinus Sylvestris Oil-based fuels [4], biodiesel [5], and natural gas, represent promising pathways to reducing fossil fuel dependence, lowering GHG, and ultimately achieving net-zero carbon emissions [6,7]. Hydrogen and ammonia, as zero-carbon energy carriers, have attracted growing attention in recent years. Owing to the distinctive nature of its molecular structure and physicochemical characteristics, hydrogen continues to pose substantial safety challenges in both storage and transportation [8].

Furthermore, combustion instabilities, including backfire and knocking, remain major obstacles to its large-scale utilization [9]. In contrast, ammonia offered several advantages as a hydrogen carrier, including easy liquefaction and transport, cost efficiency, and abundant availability. Since ammonia burned cleanly and produced no hazardous pollutants or GHG [10], it represented a highly promising candidate for use as an alternative fuel in internal combustion engines (ICEs).

Recognized as a carbon-free energy vector, ammonia ($NH_3$) holds significant potential for decarbonizing energy systems [11-13]. It is readily liquefiable at ambient temperature (298 K) under a moderate pressure of about 1 MPa, offering a volumetric energy density nearly 1.8 times higher than that of liquid hydrogen [14-16]. Currently, ammonia ranks among the most extensively produced industrial chemicals worldwide and is

Received: December 2025, Accepted: January 2026
Correspondence to: Thong Duc Hong, Ho Chi Minh City University of Technology (HCMUT), 268 Ly Thuong Kiet Street, Ho Chi Minh City, Vietnam
E-mail: hongducthong@hcmut.edu.vn
**doi: 10.5937/fme2601159H**

supported by a well-developed infrastructure for its production, storage, and distribution. Moreover, it can be synthesized from both fossil-derived and renewable resources [17,18]. Driven by the global shift toward a low-carbon economy, the ammonia industry is rapidly transforming its production pathways to become greener and more sustainable, thereby reducing both greenhouse gas (GHG) emissions and production costs. Ongoing development efforts are focused on green and blue ammonia synthesis, as well as the exploration of non-Haber–Bosch processes for sustainable ammonia production [19,20]. However, ammonia's use as an ICE fuel poses several challenges, such as its high ignition energy and required ignition temperature, slow flame propagation speed, and relatively lower adiabatic flame temperature compared to diesel. Moreover, its lower heating value (LHV) is roughly 60% less than that of conventional diesel fuel [21].

A range of studies in the current literature focuses on the use of ammonia as a fuel in reciprocating engines, encompassing both spark-ignition (SI) and compression-ignition (CI) configurations. The expanding volume of research underscores the growing interest in integrating ammonia into the energy sector as a viable fuel option. An overview of studies examining ammonia combustion and co-combustion in CI engines is provided in Table 1.

**Table 1. A comprehensive review of ammonia's role in dual-fuel compression-ignition engines: impacts on efficiency and emissions**

| Research design | Impact of Ammonia | Reference |
|---|---|---|
| 1-cylinder; $NH_3$ port injection; CR 18.5; 900-1300 rpm; $NH_3$: 20%, 50%, 60%, engine under different loads | ITEg reached up to 51.5%, similar to the diesel-only mode; $N_2O$ and NO emissions were each below 1, 7, and 6 g/kWh. | Pei et al. [22] |
| 1-cylinder; diesel pilot injection strategy; $NH_3$ energy fractions of 40%, 50%, 60%, and 70% | $NH_3$ ratio peaked at 70%; pilot injection reduced emissions to 13%; ITE reached 45%. | Mi et al. [23] |
| 6-cylinders; CR 16; 750 rpm; $NH_3$ replaced LNG with constant IMEP | Lower efficiency from slow $NH_3$ combustion; higher $NH_3$ ratio cuts CO but raises NOx. | Xu et at. [24] |
| 1-cylinder, CR 16.25; port fuel injection; ADDF; Diesel injection timing | With 40% ADDF, $NO_3$ emissions dropped by nearly 59%. | Yousefi et al. [25] |
| Low-speed marine engine; Diesel energy fractions of 1%, 5%, and 10% under full load | AER improves efficiency; earlier injection increases $NO_3$, reduces $NH_3$ slip; reduces GHG. | Liu et al. [26] |
| 1-cylinder, CR 16.25; 910 rpm; Direct $NH_3$ injection at 50% load | NO decreased 13.5%; GHG was nearly 91% lower than diesel operation. | Shin et al. [27] |
| CFR engine, CR 10; 1800rpm; DME/$NH_3$ blends at 40/60 and 60/40 ratios | optimal injection: 90–340° BTDC; soot & CO down, $NO_3$ & HRR up. | Ryu et al. [28] |

Complementing experimental investigations, simulation-based studies have played a crucial role in evaluating engine performance, with AVL BOOST emerging as one of the most validated and dependable computational tools in this field [29,30]. Due to its strong capability for user-defined fuel modeling, AVL BOOST has been widely adopted for simulating performance and emission characteristics under different alternative fuel scenarios. Aldhaidhawi et al. [31] explored ethanol–diesel blends as a strategy to mitigate greenhouse gas emissions, analyzing engine performance, gaseous emissions, and power output across varying ethanol ratios under different engine speeds. Rimkus et al. [32] investigated the addition of liquefied petroleum gas (LPG) to diesel engines, observing a decline in thermal efficiency and an increase in incomplete combustion products (CO, HC, and smoke), accompanied by reduced $NO_2$ and $CO_2$ emissions. Lasocki et al. [33] analyzed the influence of ammonia supplementation on compression-ignition engine performance, concluding that higher power and torque outputs can be achieved under certain operating conditions by introducing a fixed, limited quantity of ammonia into the diesel fuel supply. In addition to alternative fuel studies, AVL BOOST is highly effective for practical experimental work. Hong et al. [34] demonstrated this by modeling a 6-cylinder diesel engine to analyze partial-load performance for optimizing drivetrain transmission ratios. In a follow-up study, they applied the software to optimize diesel engine performance in fire pump systems, striking a balance between efficiency, cost, and environmental impact [35]. Based on evidence from prior research confirming AVL BOOST as a validated and effective thermodynamic modeling platform, it was adopted in this study for simulating the single-cylinder diesel engine.

The growing adoption of ammonia as an alternative fuel, particularly in stationary and marine engines, has stimulated extensive research aimed at evaluating key engine performance parameters through both experimental and numerical approaches [36,37]. Although previous studies listed in Table 1 report a reduction in unburned $NH_3$ emissions with increasing ammonia substitution ratios, the overall trend shows a rise in $NO_3$ emissions. This increase is likely attributable to higher in-cylinder temperatures and altered combustion chemistry associated with high ammonia fractions. In the present study, a lower ammonia energy ratio is investigated, based on the hypothesis that it can effectively mitigate $NO_3$ formation while maintaining the benefits of ammonia as a carbon-free fuel. Moreover, the influence of low-ammonia energy contribution on traditional CI engines has not yet been comprehensively investigated in existing studies. This research gap in investigating ammonia at low energy fractions is expected to lead to significant differences in the combustion process and emissions of agricultural engines, consequently causing variations in the torque and power output of stationary engines. The findings from this research are expected to apply to agricultural contexts, where such engines are widely used. A stationary engine is selected over an automotive engine for two key reasons: First, agricultural

machinery typically operates at steady load and speed conditions, closely matching the stable operating point of stationary engines. This stability facilitates better control and optimization of combustion when using alternative fuels, such as ammonia. Second, emission regulations in agricultural applications are generally less stringent than those for on-road vehicles, providing a more feasible environment for the initial deployment of carbon-free fuels such as ammonia. Although experimental methods offer high accuracy and reliability in assessing engine performance, they are typically limited by considerable time demands, elevated costs, fuel consumption, and the scarcity of qualified operators. Alternatively, computa–tional simulations offer a practical and economical solution for evaluating engine performance across mul–tiple conditions, providing valuable insights into operational behaviors that are otherwise challenging to examine experimentally.

This work investigates the diesel-ammonia blend in a Vikyno RV125_2 single-cylinder stationary diesel engine at different blend ratios of 2%, 4%, 6%, 8%, and 10%. The engine was modeled with AVL BOOST soft–ware and validated using experimental data to ensure the accuracy of the simulation. Focusing on an 85% load as representative of the steady-state duty cycle for small stationary engines, this study targets a high-load operating point that is not only relevant for practical generator applications but also eliminates the issues of low-load instability and incomplete combustion com–monly encountered in dual-fuel engines [38]. The selec–tion of three combustion durations in this study was guided by a previous study, ensuring they represent conditions within the stable operational envelope of a stationary compression-ignition engine [39]. The am–monia substitution ratio was determined on an energy-equivalent basis to ensure a fair comparison between liquid and gaseous fuels. A range of 0–10% was selected to address a research gap, as previous studies have not investigated this range of energy ratios. This range is considered sufficient to evaluate ammonia's influence on combustion characteristics. This paper aims to assess the impact of ammonia-diesel blend ratios on the combustion process, engine performance, and exhaust emissions for small-scale stationary appli–cations. Furthermore, these results serve as a practical reference for researchers and engineers seeking to develop cleaner, economically viable, and environ–mentally sustainable energy solutions for stationary diesel engines operating under high-load conditions.

## 2. MATERIALS AND METHODS

### 2.1 Stimulation engine

The model of dual fuel was constructed in AVL BOOST (Figure 1) and parameterized according to the specifications of the Vikyno RV 125_2 (Table 2). In the proposed model, E1 represents the Diesel-NH3 engine; CL1 denotes the air cleaner. Five measuring points, MP1-MP5, are utilized to monitor gas states and flow data. Flow restriction elements R1–R3 are used to model targeted pressure drops at designated points in the piping system. SB1 and SB2 represent the boundary conditions.

Additionally, building upon the standard AVL BOOST engine model, a new subsystem was implemented to simulate the introduction of ammonia at a controlled blend ratio. The ammonia supply is modeled via a dedicated injector (I1) installed in the intake runner. Strategically located downstream of flow resistor R2, the injector's output is monitored by measuring point MP3, which provides the feedback necessary for precise dosage control before the mixture enters cylinder C1.

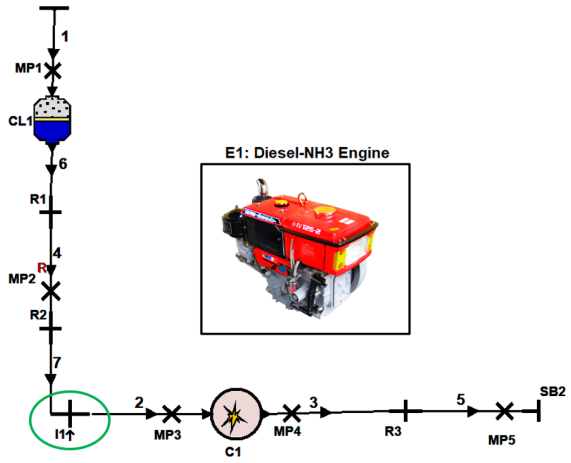


**Figure 1. 1D simulation model**

**Table 2. Engine model specifications [40]**

| | |
|---|---|
| Engine model | Vikyno RV125-2 |
| Type of engine | Single-cylinder, 4-stroke, CI |
| Geometry | 624 cm³ (Swept volume)<br>94 × 90 mm (bore × stroke)<br>18:1 (compression ratio) |
| Performance | 12.5 HP @ 2400 rpm<br>4.04 kg·m @ 1800 rpm |

The key thermophysical and chemical characteristics of both fuels are summarized in Table 3. Containing 17.6% hydrogen by weight, ammonia is a promising medium for storing and transporting hydrogen. Its absence of carbon ensures that combustion generates no carbon compounds, positioning it as a clean and environmentally friendly energy source. While ammonia's energy density is lower than that of conventional hydrocarbon fuels, its high autoignition resistance renders it suitable for high-compression scenarios and valuable as an octane-enhancing additive. Notably, ammonia's latent heat of vaporization (1370 kJ/kg) far exceeds that of diesel (232.4 kJ/kg), signifying a significantly greater energy demand from the surroundings during vaporization. Additionally, its lower heating value of 18.6 MJ/kg is approximately half that of diesel fuel (42.8 MJ/kg), as detailed in the same table [41]. In the present study, RAE is defined as the ratio of the energy derived from ammonia to the total energy input in the dual-fuel model [42,43]

$$RAE = \frac{\dot{m}_{NH_3} \times LHV_{NH_3}}{\dot{m}_{diesel} \times LHV_{diesel} + \dot{m}_{NH_3} \times LHV_{NH_3}} \quad (1)$$

where $m_{NH3}$ and $m_{diesel}$ represent the mass of ammonia (to the intake manifold) and the mass of diesel fuel (injected to the cylinder per cycle). The corresponding lower heating values are $LHV_{NH3}$ and $LHV_{diesel}$. The precise mass and energy values applied in this analysis are listed in Table 4.

**Table 3. Key characteristics of ammonia and diesel [41]**

| Property | Ammonia | Diesel |
|---|---|---|
| Lower heating value (MJ/kg) | 18.6 | 42.8 |
| Density @ 25°C, 1 bar (kg/m$^3$) | 0.178 | 849 |
| Latent heat of vaporization (kJ/kg) | 1370 | 232.4 |
| Laminar burning velocity (m/s) | 0.07 | 0.86 |
| Adiabatic flame temperature (°C) | 1800 | 2300 |

**Table 4. Mass and energy proportions in diesel-ammonia blends**

| | Diesel/cycle | | $NH_3$/cycle | | Mixture | |
|---|---|---|---|---|---|---|
| | $m_{Diesel}$ (mg) | $Q_{Diesel}$ (J) | $m_{NH3}$ (mg) | $Q_{NH3}$ (J) | $m_{mix}$ (mg) | $Q_{mix}$ (J) |
| 0RAE | 29.00 | 1241.20 | 0 | 0 | 29.00 | 1241.2 |
| 2RAE | 28.42 | 1216.38 | 1.33 | 24.82 | 29.75 | 1241.2 |
| 4RAE | 27.84 | 1191.55 | 2.67 | 49.65 | 30.51 | 1241.2 |
| 6RAE | 27.26 | 1166.73 | 4.00 | 74.47 | 31.26 | 1241.2 |
| 8RAE | 26.68 | 1141.90 | 5.34 | 99.30 | 32.02 | 1241.2 |
| 10RAE | 26.10 | 1117.08 | 6.67 | 124.12 | 32.77 | 1241.2 |

### 2.2 Combustion and heat transfer models

The cylinder combustion process is simulated via the "Vibe 2-zone" model. This approach partitions the cylinder volume into two regions: a burnt zone and an unburnt zone. For simulation purposes, each zone is considered spatially uniform in terms of pressure, temperature, and species concentration at any given time. The system is modeled as closed between intake valve closure and exhaust valve opening, with thermodynamic homogeneity maintained separately within each zone. The model is based on several key assumptions: instantaneous uniform cylinder pressure, no inter-zone heat transfer, ideal-gas behavior with thermal properties derived from relations for an air–natural gas mixture, and—for fuel blends—simultaneous direct injection of ammonia and diesel through a standard injection system.

According to these assumptions, sub-models for each zone are zero-dimensional. The First Law of Thermodynamics gives the state of the cylinder for the burnt zone as follows in a general form [44]:

$$\frac{d(m_b u_b)}{da} = -p_c \frac{dV_b}{da} + \frac{dQ_F}{da} - \sum \frac{dQ_{wb}}{da} + h_u \frac{dm_b}{da} - \frac{h_{BB,b} dm_{BB,u}}{da} \quad (2)$$

Energy conservation in the unburnt zone is presented as Eq. (3):

$$\frac{d(m_b u_b)}{da} = -p_c \frac{dV_u}{da} - \sum \frac{dQ_{wu}}{da} - h_u \frac{dm_b}{da} - \frac{h_{BB,u} dm_{BB,u}}{da} \quad (3)$$

where $Q_F$ and $\alpha$ denote the total combustion heat release and the crank angle, respectively, the term $h_u(dm_b/d\alpha)$ represents the enthalpy transfer from the unburned to the burned zone, where $m_b$ and $m_u$ are the burned and unburned masses, and $h_{BB}$ is the blow-by enthalpy. In Eqs. (2) and (3), the sum of the burned and unburned zone volumes equals the cylinder volume:

$$V = V_u + V_b \quad (4)$$

Thus, the sum of the volumetric changes for each zone equals the change in total cylinder volume.

$$\frac{dV_b}{da} + \frac{dV_u}{da} = \frac{dV_c}{da} \quad (5)$$

Heat transfer inside internal combustion engines involves convective and radiative mechanisms. While radiative heat transfer contributes only 3–4% of the total heat loss in SI engines, it may increase to around 10% in diesel engines due to soot formation during combustion.

The convective heat transfer between the in-cylinder gases and the combustion chamber walls is highly non-uniform and transient, posing a fundamental challenge for accurate modeling. To address this complexity, the Woschni (1978) correlation is commonly adopted as a simplified yet practical approach for estimating heat loss, particularly during the high-pressure combustion stage [45]. Due to its straightforward formulation, computational efficiency, and reasonable accuracy across a wide range of engine types, it has been extensively used in research. For instance, Thong et al. employed this model to compare the combustion, performance, and emissions of the VB2Z and M-VB2Z combustion models in a diesel engine, while another study applied it to analyze the effects of LPG-diesel blends on the performance, combustion, and emissions of a stationary diesel engine [46,47]. The following expression gives its formulation:

$$Q_w = A_i \alpha_w (T_c - T_{wi}) \quad (6)$$

where $Q_w$ is the wall heat loss, $A_i$ is the surface area, $\alpha_w$ is the heat transfer coefficient, $T_c$ is the cylinder gas temperature, and $T_{wi}$ is the wall temperature.

$$a_w = 130 \cdot D^{-0.2} \cdot p_c^{0.8} \cdot T_c^{-0.53} \cdot \left[ C_1 C_m + C_2 \frac{V_D T_{c,1}}{p_{c,1} V_{c,1}} \cdot (p_c - p_{c,0}) \right]^{0.8} \quad (7)$$

The Eq (7) variables comprise the instantaneous thermodynamic state: cylinder temperature $T_c$, cylinder pressure $p_c$, along with the geometric parameter of bore diameter $D$. Engine operation is characterized by the mean piston speed $C_m$ and the flow-dependent coefficient $C_1$, while $C_2$ is a fitted constant. Initial conditions are given by the temperature $T_{c,1}$ and pressure $p_{c,1}$ at inlet valve closing, with the system geometry defined by the instantaneous volume $V$. The term $p_{c,0}$ serves as the reference motored pressure.

### 2.3 Simulation description

This study utilizes the Vibe function to characterize the combustion process, which is defined by four governing parameters: the start of combustion (SOC), combustion duration, a profile-defining shape factor, and a fuel-

mass-burned fraction coefficient. Simulations were conducted at a constant 85% engine load with speeds ranging from 900 to 2400 rpm in 300 rpm increments. The optimal diesel ignition timing was selected from a combustion duration range of 80° to 120°, following the approach of Hong et al. [48]. Although ammonia generally prolongs ignition delay in diesel–ammonia dual-fuel combustion owing to its low chemical reactivity, E. Nadimi et al. [49] observed no significant change in ignition delay over ammonia blending ratios of 0 to 14.9%. In line with this finding, the SOC was modelled using fixed crank angles of −7°, −11°, and −15° CA for the CD80, CD100, and CD120 cases, respectively. The Vibe shape factor was consistently set to 0.55 for all scenarios. An efficiency factor (a) of 6.9 was applied, corresponding to the assumption of complete combustion across all simulated conditions.

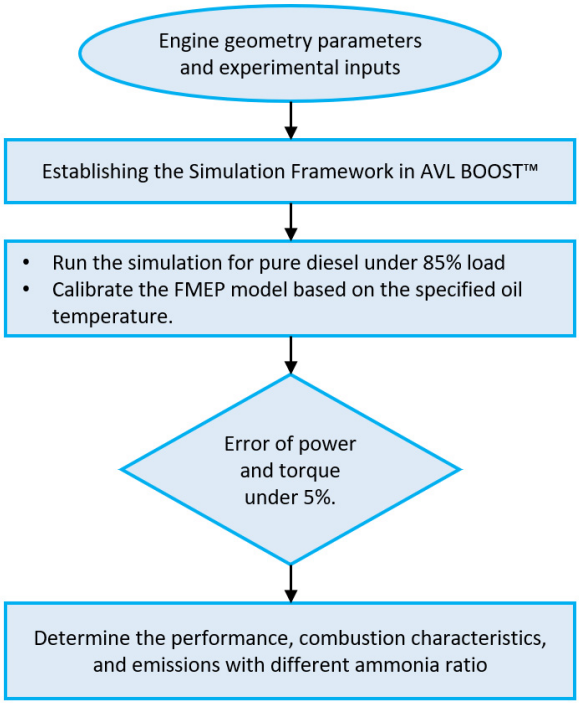


**Figure 2. Simulation procedure for an RV 125-2 engine fueled with diesel-ammonia blends using AVL BOOST**

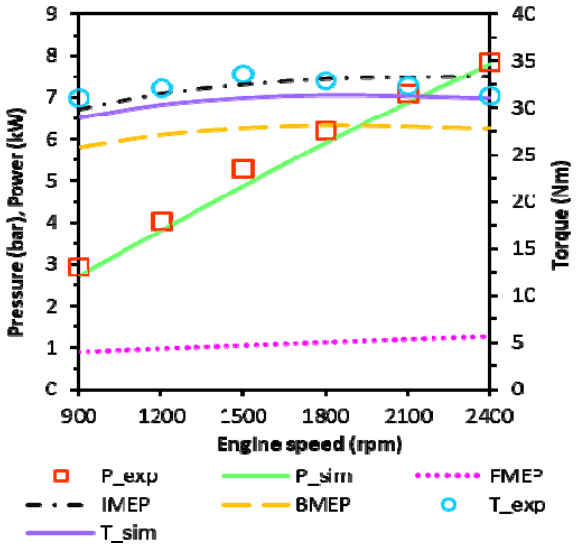


**Figure 3. Calibration of power and torque at 85% load**

The overall simulation procedure, including evaluation of model accuracy and validity, is illustrated in Figure 2. In this process, experimental output data obtained from testing an RV 125-2 engine on a test bed were used to validate the AVL BOOST model [48]. The results were expressed as trendline approximation functions corresponding to fixed fuel quantities per cycle. These findings are employed in the present study to confirm the accuracy of the numerical model. A key step in this procedure is calibrating the FMEP model, which depends on the type of oil and the viscosity-temperature of the lubricant. Frictional losses, representing the difference between indicated work and sound brake output, reduce net engine efficiency, increase specific fuel consumption, and accelerate mechanical wear. Because the accurate estimation of friction losses remains challenging, empirical methods, such as motored engine testing, remain essential, highlighting the need for more comprehensive modeling in engine design and development [50].

In this work, engine friction is calculated using the method developed by Shayler, Leong, and Murphy (SLM), which accounts for frictional losses in the main bearings, valve train, piston assembly, and auxiliary systems. The SLM model is applied to analyze friction losses under low-temperature and low-speed conditions as part of an investigation into cold-start performance [51]. The experimental and simulated torque, power, BMEP, FMEP, and IMEP values, plotted against engine speed under an 85% load, are presented in Figure 3. In the figure, P_exp and T_exp denote the experimental power and torque outputs, while P_sim and T_sim represent the simulated power and torque obtained after applying the friction mean effective pressure (FMEP) model. The indicated mean effective pressure (IMEP), brake mean effective pressure (BMEP), and FMEP were calculated using an AVL-based mathematical model to assess engine performance. The simulation results demonstrate strong agreement with the experimental data, with a maximum error margin of less than 5%, validating the accuracy of the applied model.

The (FMEP) is presented as follows [52]:

$$FMEP_{total} = \left(FMEP_{CS} + FMEP_{p} + FMEP_{VT} + FMEP_{AUX} + FMEP_{IP}\right)\left(\frac{v_{T_{oil}}}{v_{T_{oil}=90°}}\right)^{0.24} \quad (8)$$

where $FMEP_{CS}$, $FMEP_{p}$, $FMEP_{VT}$, $FMEP_{AUX}$, $FMEP_{IP}$, denote the frictional mean effective pressures associated with the crankshaft, reciprocating assembly, valve train, auxiliary, and cam follower, respectively. This term accounts for the variation in oil viscosity with temperature.

## 3. RESULTS AND DISCUSSIONS

### 3.1 Influence of diesel-ammonia blend proportions on combustion behavior

Figure 4 shows the in-cylinder pressure profiles for combustion using pure diesel as the reference case and for the co-combustion of diesel with ammonia at an engine speed of 2400 rpm. At the CD80 phase, two

distinct trends are observed. First, diesel–ammonia blends exhibit a higher peak of HRR than the reference diesel fuel at 2400 rpm. Specifically, at 2400 rpm, it increases incrementally from 40.09 J/deg (0RAE) to 40.77 J/deg (10RAE). Second, the peak of HRR is slightly delayed with increasing ammonia content. Compared to the 0RAE baseline, the delay from 0.5 to 1.5 crank angle degrees ($^0$CA) for the 2RAE through 10RAE blends at 2400 rpm. Due to its high reactivity, diesel acts as the primary ignition source. The estab–lished ignition kernels enhance the propagation of diesel combustion and concurrently initiate the oxidation of the premixed ammonia-air charge [53].

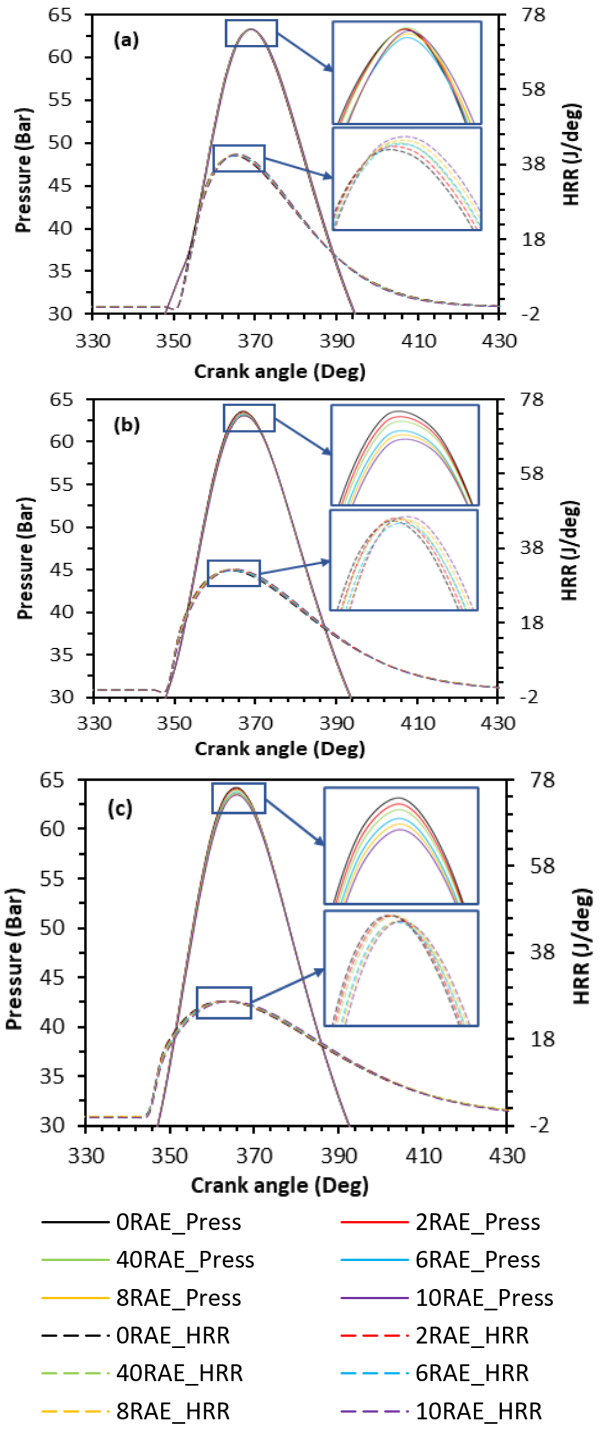


**Figure 4. In-cylinder pressure and heat release rate at 85% load for ammonia–diesel blends at 2400rpm: (a) CD80, (b) CD100, and (c) CD120.**

In the CD80 operating condition (SOC is equally 7bTDC), the extended ignition delay allows better diesel–air premixing before autoignition. Since ammo–nia is already fully premixed via port injection, diesel reliably ignites the ammonia–air mixture, causing a larger portion of the charge to burn rapidly upon ignition. This intensifies premixed combustion, resul–ting in a higher HRR peak across all ammonia blending ratios. The increased total heat released during this con–centrated phase leads to a higher peak of in-cylinder pressures compared to the 0RAE baseline. The pres–sures for 2RAE and 4RAE increase slightly to 63.37 and 63.38 bar, whereas the pressures for 6RAE, 8RAE, and 10RAE exhibit very slight decreases to 63.29, 63.32, and 63.35 bar, respectively.

In the CD100 case, the maximum HRR for ammonia blends shows a slightly retarded crank angle relative to pure diesel, with delays increasing progressively with the ammonia fraction. The crank angle at maximum HRR increased from 0.8 to 2.8 degrees for the 10RAE blend at 2400 rpm, respectively; however, the HRR value at this phase remained unchanged. This behavior can be explained by the shorter ignition delay and premixed combustion period at CD100, resulting in a lower and later peak of HRR compared to the CD80 condition. The pressure decreased by 0.11, 0.22, 0.4, 0.5, and 0.6 bar at 2400 rpm for the respective blends.

A similar trend is observed under CD120 conditions, with both a slight reduction and a retardation in the heat release rate. Specifically, the 10RAE blend exhibits a 2.0°CA delay and a 2.2 J/deg decrease in the peak of HRR compared to pure diesel. Cylinder pressure also declines with increasing ammonia content. At 2400 rpm, the reductions are 0.15, 0.29, 0.52, 0.66, and 0.80 bar, respectively. Thus, it is evident that ammonia affects the peak of in-cylinder pressure. Combustion begins before TDC, which lowers the rate of heat release and results in some energy loss during piston compression, contributing to the reduction in the pres–sure trace [54]. Furthermore, the phase after the peak of pressure increases with the ammonia ratio, even if the peak of pressure is higher. This is because when diesel ignites, it initiates the combustion of $NH_3$, which subse–quently raises the pressure.

Figure 5 shows the in-cylinder temperature varia–tions for a range of diesel-ammonia mixture ratios at three different combustion times under 85% load, which illustrates the temperature reduction associated with higher $NH_3$ substitution ratios. Analysis shows that while ammonia blending leads to a measurable reduc–tion in peak combustion temperature, the magnitude of this effect is negligible. This demonstrates a consistent decrease in 10RAE compared to 0RAE across engine speeds.

At 2400 rpm, the peak of temperature decreases by 0.77%, 1.07%, and 1.38% for CD80, CD100, and CD120, respectively. These reductions are primarily attributable to ammonia's distinct oxidation kinetics, which are influenced by its strong molecular polarity and reflected in its laminar burning velocity. This velo–city is maximized at a slightly rich equivalence ratio ($\lambda \approx 0.9$) and falls off markedly as the mixture becomes either richer or leaner [55]. Additionally, the tempe–

rature decrease is associated with longer combustion durations. The extended combustion duration spreads heat release over a wider crank angle range, suppressing the formation of a distinct temperature peak. Because heat is partially released during the expansion stroke, the effective temperature rise is diminished, resulting in lower cylinder temperatures.

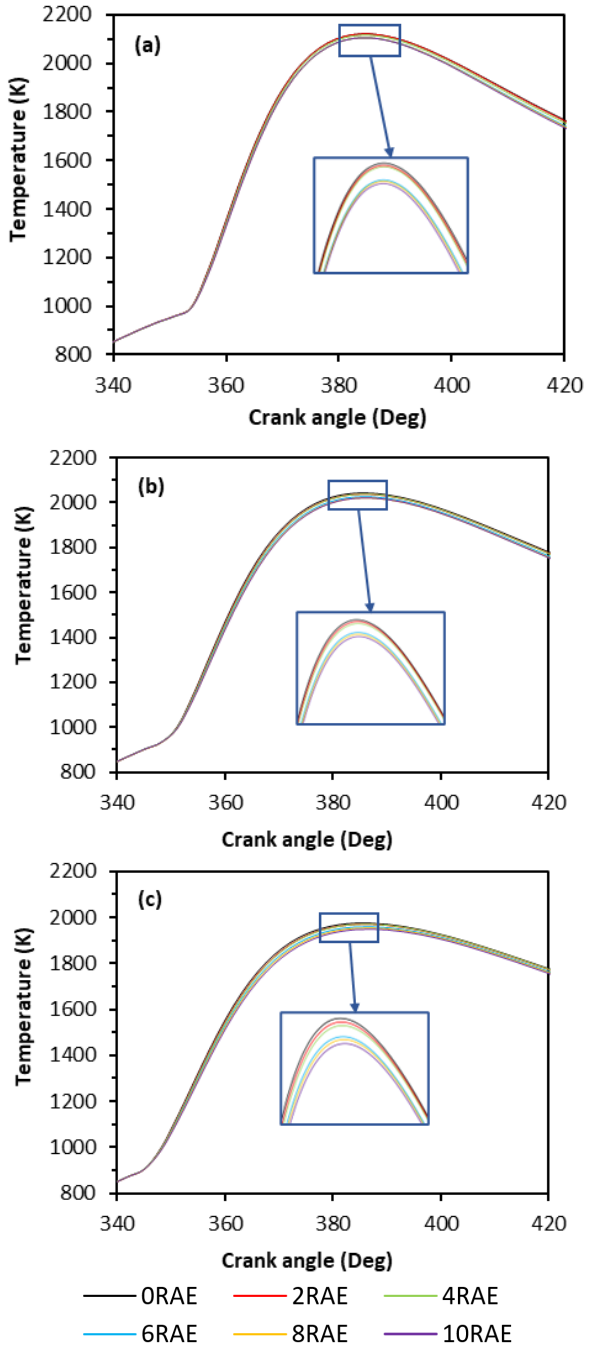


**Figure 5. In-cylinder temperature at 85% load for ammonia–diesel blends at 2400rpm: (a) CD80, (b) CD100, and (c) CD120.**

### 2.4 Influence of diesel-ammonia blend proportions on engine performance

Figure 6 depicts the effect of ammonia substitution ratio on torque and power at various combustion durations with 85% load. Overall, both torque and power improve as the ammonia ratio increases across all three combustion duration situations, with peak performance consistently achieved between 1600 and 1800 rpm. At 1800 rpm, for example, the torque output of 10RAE rises 1.03, 1.08, and 1.07% at CD80, CD100, and CD120, respec–tively, and the power output of 10RAE increases by 1.04, 1.03, and 0.98% for CD80, CD100, and CD120. The underlying mechanism involves two key factors. First, although the peak of HRR is lower than that of pure diesel, the diesel-ammonia blend sustains a higher pressure after this peak and throughout the later stages of the combustion process. This results in more complete combustion, and the greater heat released in these later stages boosts overall efficiency. Second, diesel-ammonia com–bustion exhibits lower in-cylinder temperatures, which reduces heat transfer losses through the cylinder walls [56].

Furthermore, combustion duration is a crucial parameter that significantly influences engine perfor–mance; extended combustion duration results in dimini–shed power and torque output. The underlying reason is that a prolonged burn reduces the heat release rate and lowers combustion efficiency, which directly limits the engine's power and torque.

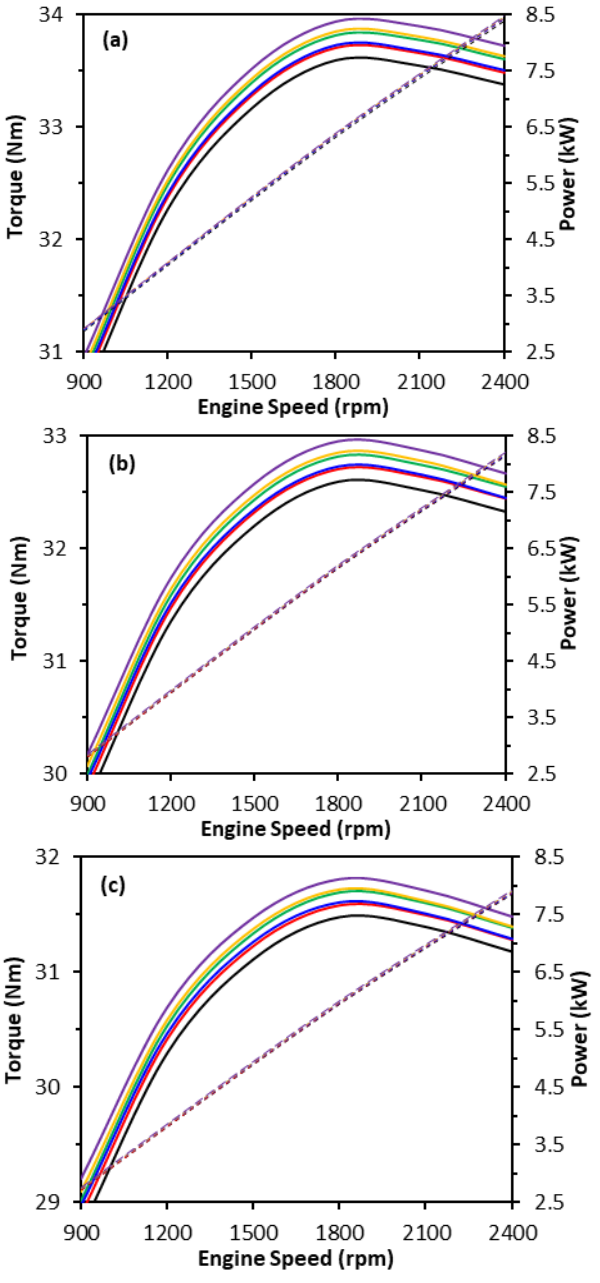

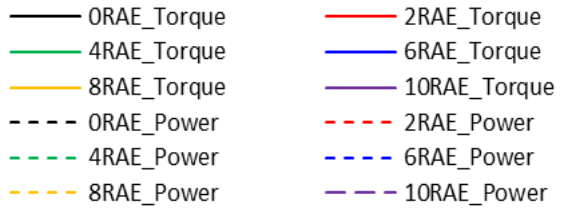


**Figure 6. Power and torque at 85% load for ammonia–diesel blends: (a) CD80, (b) CD100, and (c) CD120.**

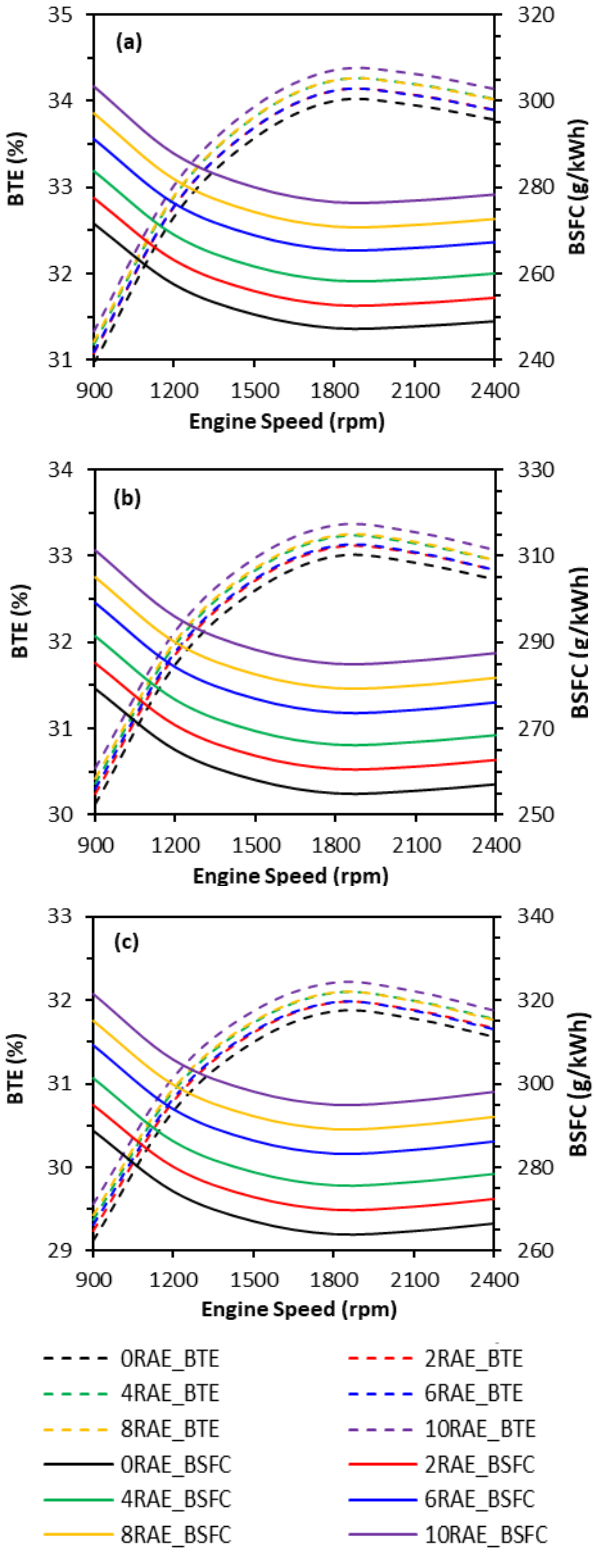


**Figure 7. BTE and BSFC at 85% load for ammonia–diesel blends: (a) CD80, (b) CD100, and (c) CD120.**

Figure 7 illustrates the variation in brake thermal efficiency (BTE) and brake specific fuel consumption (BSFC) with engine speed for different diesel-ammonia blends under an 85% load. While BSFC generally declines with rising engine speed, the overarching trend reveals higher fuel consumption as more ammonia is added. At 1800 rpm, measured BSFC values for the blends (2RAE to 10RAE) show sequential increases of 2.2%, 4.26%, 6.77%, 8.64%, and 10.5% relative to the baseline 0RAE. Ammonia has a lower calorific value (18.6 MJ/kg) than diesel (42.8 MJ/kg), so more ammonia must be injected to deliver the same energy input, resulting in a higher BSFC. In general, the data from CD100 and CD120 generally indicate a greater across all speed ranges. This is to be expected since longer combustion times typically result in higher fuel usage, albeit the increase is still relatively modest. Still, higher ammonia shares are required to achieve the desired power output, resulting in increased fuel consumption at all speeds.

Simulation results indicate that increasing the ammonia contribution in the diesel–ammonia blend yie–lds only a modest improvement in BTE, consistently observed across all tested engine speeds. At constant energy input, ammonia blends produce slightly higher brake power than pure diesel operation. Moreover, the improvement likely arises from enhanced combustion characteristics of the ammonia-diesel mixture, which increases the engine's ability to convert thermal input into practical work. These properties include greater fuel-air premixing and a more uniform combustion process.

### 2.5 Influence of diesel-ammonia blend proportions on emissions

The influence of $NH_3$ on NOx under 85% load condi–tions is shown in Figure 8. It is evident that increasing the ammonia blending ratio significantly reduces NOx emissions at all engine speeds. For CD80, at 2400 rpm, NOx emissions for 2RAE, 4RAE, 6RAE, 8RAE, and 10RAE decrease by 3.66%, 7.2%, 15.11%, 18.35%, and 22.24%, respectively, compared with pure diesel. This reduction can be attributed to two primary factors. First, the addition of $NH_3$ reduces the in-cylinder combustion temperature, directly suppressing thermal NO produc–tion, as the rate of this reaction depends exponentially on temperature. Moreover, port-injected ammonia low–ers the air-to-fuel ratio, thereby increasing the equiva–lence ratio ($\Phi$) and creating conditions that further inhibit NO formation. Secondly, $NH_3$ participates in the fuel-NO pathway, where it undergoes dehydrogenation via thermal decomposition or reactions with OH, H, and O radicals in the cylinder to form $NH_2$ radicals [57].

In the temperature range of 450–925 K, these $NH_2$ radicals react primarily with oxidizers like $HO_2$ to form $H_2NO$, which subsequently decomposes to HNO. According to the fuel-NO mechanism, nitric oxide (NO) is ultimately produced when HNO reacts with oxygen ($O_2$). This pathway represents a potential source of increased NO emissions from the co-combustion of ammonia and diesel. Concurrently, ammonia-derived radicals engage in NO-reduction chemistry. In the temperature range between 1100 and 1400 K, a

chemical de-NOx reaction occurs between $NH_2$ radicals and the NO formed. However, some byproducts of these reactions can be partially re-oxidized to NO. At temperatures above 1400 K, NH radicals (from further dehydrogenation of $NH_2$) can reduce NO to form $N_2O$. These reduction pathways also generate N and $N_2$ radicals, which, at temperatures exceeding 1600 K, participate in and influence the thermal Zeldovich (thermal-NO) mechanism [55].

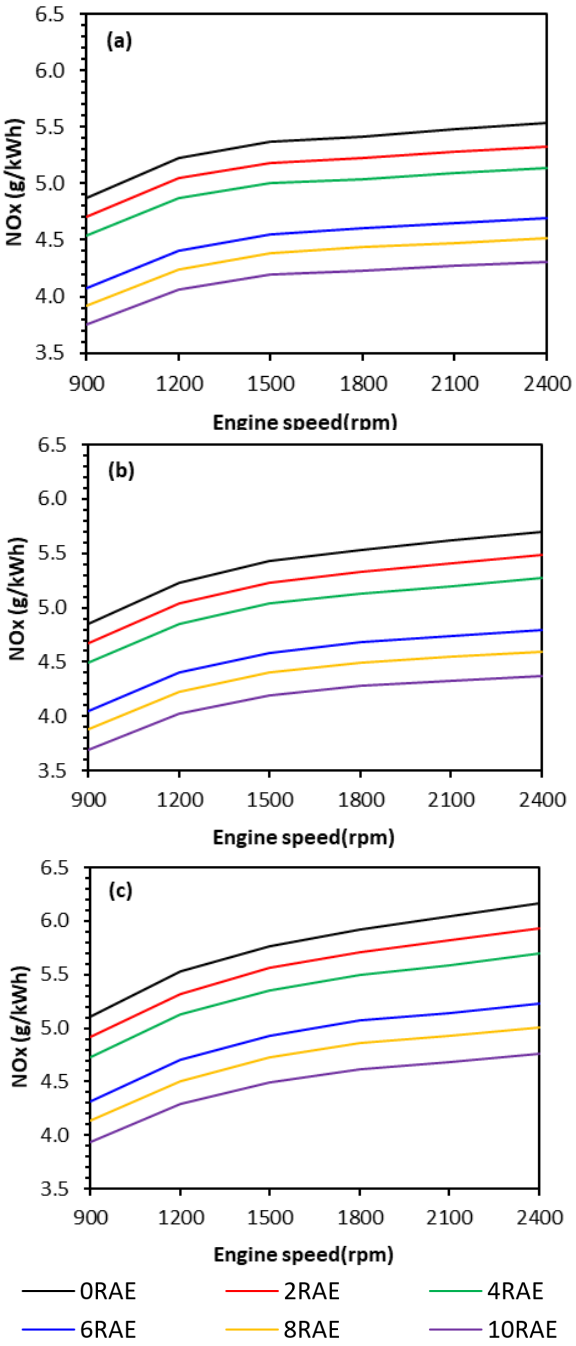


**Figure 8. NOx emissions at 85% load for ammonia–diesel blends: (a) CD80, (b) CD100, and (c) CD120.**

Combustion duration is a critical parameter that influences engine emissions, as clearly demonstrated in Figure 8, where NOx levels increase with longer combustion durations. This positive correlation can be attributed to two combined effects. First, the extended duration increases the residence time of gases at high temperatures, allowing more time for the thermally driven NOx formation reactions to progress. Second, although a longer burn may lower the peak temperature, it can lead to a more gradual depletion of oxygen over the expansion stroke. This maintains locally favorable conditions (adequate oxygen availability at elevated temperatures) for NO formation over a more extended period, resulting in higher cumulative NOx emissions.

Carbon monoxide (CO) forms in high-temperature, fuel-rich zones within the combustion chamber, resul–ting primarily from incomplete combustion under con–ditions of low local temperature and insufficient oxygen [58]. Figure. Figure 9 illustrates the impact of ammonia content on CO emissions at various engine speeds, demonstrating that CO emissions decrease with increasing ammonia blending ratios, yet exhibit a complex relationship with engine speed. The lowest CO emissions occur at 1500 rpm and CD80. For the 2RAE, 4RAE, 6RAE, 8RAE, and 10RAE blends, CO emissions are 0.021, 0.0197, 0.0174, 0.0164, and 0.0154 g/kWh, respectively, corresponding to reductions of 5.98%, 11.56%, 16.93%, 21.81%, and 26.34% compared to 0RAE.

It clearly indicates that ammonia blending is effective at reducing CO emissions across all engine speeds. While higher $NH_3$ blending ratios consistently reduce CO at any given speed, the influence of engine speed reveals a dual mechanism. At low speeds (900–1200 rpm), the extended combustion duration allows the chemical benefits of ammonia to dominate: its decom–position supplements oxygen radicals, dilutes the carbon content of the fuel, and promotes more premixed com–bustion—all of which enhance CO oxidation [59]. In contrast, at medium to higher speeds (1800–2400 rpm) and with higher $NH_3$ fractions, the drastically reduced time available for combustion becomes the limiting factor. Here, the inherently slower combustion kinetics of $NH_3$ outweigh its chemical advantages. The shor–tened combustion phase leads to incomplete oxidation of both diesel and ammonia, which not only leaves unburned intermediates but also disrupts the local oxidation environment, ultimately hindering the final conversion of CO to $CO_2$ and resulting in the observed rise in CO emissions.

Additionally, the results in Figure 9 also indicate that combustion duration has little influence on CO emission levels. To explain that, in a diesel engine, fuel is injected directly into the hot compressed air. The large fuel droplets vaporize, creating localized fuel-rich cores around the injector nozzles. In these regions, the air-to-fuel ratio is very low, with nearly insufficient oxygen. The oxidation of CO to $CO_2$ depends on the diffusion and mixing of these rich zones with the sur–rounding oxygen-rich charge. Consequently, the rate of mixing is the critical factor determining final CO levels while the total combustion duration has a limited effect.

The influence of diesel-ammonia blend ratio and combustion duration on soot emissions as a function of engine speed is depicted in Figure 10. Soot tends to increase slightly with increasing ammonia ratios at low engine speeds. At 900 rpm, the 10RAE blend produced 2.74%, 3.88%, and 4.14% higher soot emissions than pure diesel under CD80, CD100, and CD120 conditions, respectively.

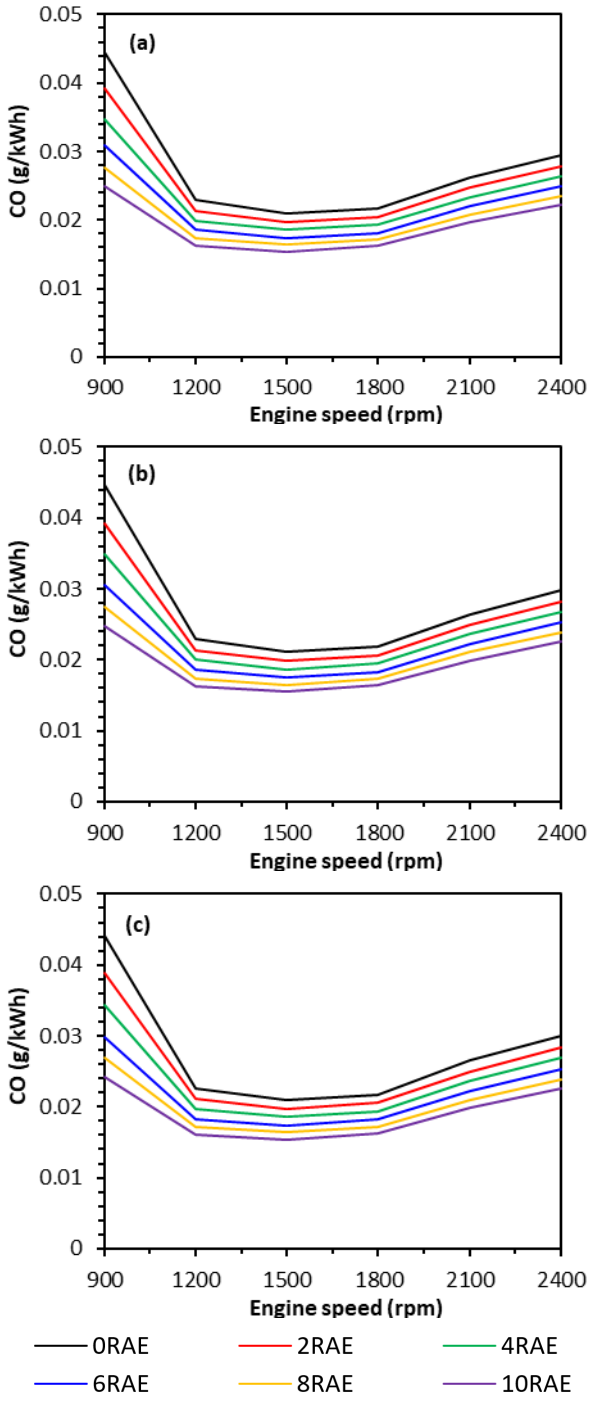


**Figure 9. CO emissions at 85% load for ammonia–diesel blends: (a) CD80, (b) CD100, and (c) CD120.**

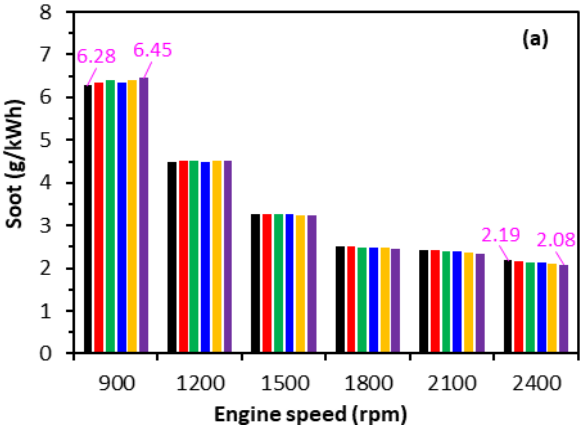


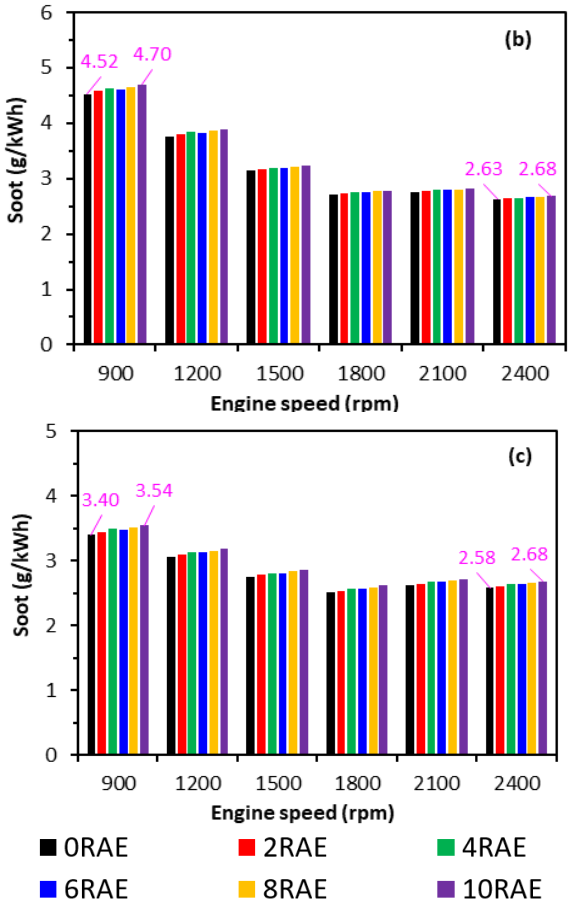


**Figure 10. Soot emissions at 85% load for ammonia–diesel blends: (a) CD80, (b) CD100, and (c) CD120.**

While $NH_3$ acts as a carbon diluent, its presence also lowers the overall combustion temperature. This temperature reduction can slow down the critical post-flame oxidation of soot particles by OH radicals, allowing a small fraction to survive. However, this negative effect is marginal because the carbon dilution benefit of $NH_3$ partially offsets it.

In contrast, at medium and high engine speeds, soot emissions exhibit only minor changes with increasing ammonia ratios. At 2400 rpm, the 10RAE blend reduces soot by 4.9% under CD80, shows no significant change under CD100, and increases by 2.68% under CD120, relative to pure diesel. Here, the enhanced in-cylinder turbulence at higher speeds drastically improves air-fuel mixing, thereby suppressing the formation of fuel-rich zones that are essential for soot nucleation. This physical effect synergizes perfectly with the chemical benefits of ammonia: carbon dilution, additional OH radical supply for soot oxidation, and alteration of soot precursor pathways. Consequently, the soot-suppression mechanisms of $NH_3$ become dominant, leading to a net reduction in emissions.

Combustion duration also plays a crucial role in soot formation during the co-combustion of diesel and ammonia. As observed, the shorter combustion duration (CD80) produces noticeably higher soot levels than the longer durations (CD100 and CD120). Although longer combustion durations are associated with lower pressure and heat release rates compared to CD80, they significantly extend the diffusion combustion phase. This provides more time for the fuel-rich zones (which are the

source of soot) to diffuse and mix with the surrounding oxygen-rich compressed air. Consequently, the former soot has sufficient time to be exposed to oxidizing agents ($O_2$, O, and most importantly, OH radicals) at high temperatures, allowing it to be fully oxidized to $CO/CO_2$ within the cylinder before being exhausted [60].

## 4. CONCLUSIONS

This study examined the effects of ammonia content on the performance, combustion characteristics, and emissions of a dual-fuel ammonia diesel engine. The analysis was conducted using a comprehensive numerical simulation model, supported by AVL BOOST software, which is designed explicitly for single-cylinder engines. The simulation covered the ratios of ammonia energy (RAE) in dual-fuel blends from 0 to 10% at 85% engine load, with three different combustion durations of 80, 100, and 120 crank angle degrees (CD80, CD100, and CD120). The significant findings of this research are summarized as follows:

- The addition of ammonia to the fuel blend consistently retarded the peak of heat release rate (HRR), in-cylinder pressure, and temperature by 1.5 to 2.8 crank angle degrees compared to pure diesel, depending on combustion duration and engine speed.
- For 10RAE, the peak of HRR increased modestly by 0.69 J/deg at CD80, remained nearly unchanged at CD100, and decreased slightly by 2 J/deg at CD120 compared to the diesel counterpart.
- The maximum pressure was slightly reduced when ammonia was added to the co-combustion process, and the degree of this reduction increased with increasing combustion time. At CD80, the maximum pressure remained nearly unchanged. However, as the combustion duration increased, the pressure decreased progressively with the increase in the ammonia fraction. At 2400 rpm, the maximum pressure showed a slight decline from 0.60 to 0.11 bar at CD100 and from 0.80 to 0.15 bar at CD120 for the 2RAE to 10RAE blends, respectively.
- Replacing diesel with $NH_3$ resulted in a consistent reduction in the peak of in-cylinder temperatures across all combustion durations and engine speeds. At 2400 rpm, the decreases were 0.77%, 1.07%, and 1.38% for CD80, CD100, and CD120, respectively.
- A higher ammonia fraction led to modest improvements in torque and power. At 1800 rpm, the 10RAE blend increased torque and power by 1.03–1.08% across the investigated combustion duration range (CD80–CD120). Additionally, brake-specific fuel consumption (BSFC) rose by 2.2% to 10.5% for the 2RAE to 10RAE blends compared to the reference fuel (0RAE).
- The NOx, CO, and soot emissions exhibited different behaviors at varying engine speeds, ammonia substitution ratios, and CDs. NOx emissions were significantly reduced by 22.24% under CD80 and 2400 rpm for 10RAE (3.75 g/kWh) compared to 0RAE (4.87 g/kWh). CO emissions also decreased progressively with higher ammonia blending ratios. 10RAE produced 0.0154 g/kWh of CO emissions, which is approximately 27% lower than the 0.021 g/kWh recorded for 0RAE at 1500 rpm. Soot emissions exhibited a slight upward trend at low engine speed (900 rpm); however, at higher engine speeds, ammonia energy blends showed reduced soot emissions, which remained relatively stable. Moreover, under the longer combustion duration (CD120), a slight increase in soot was observed with ammonia addition, at 2400 rpm, soot emissions for 10RAE were 4.14% higher than those for 0RAE.

This study highlights the potential of using ammonia diesel dual-fuel systems in stationary engines to support rural development in Vietnam, aiming to successfully reconcile performance with reduced greenhouse gas emissions. Future work should focus on optimizing the start of combustion for various RAE in dual-fuel blends to further enhance engine performance and emission characteristics. Additionally, a comparison of ammonia with other carbon-free alternative fuels, such as hydrogen, is also a potential area of research that could provide a broader perspective on their relative benefits in dual-fuel systems.

## ACKNOWLEDGMENT

We acknowledge the Ho Chi Minh City University of Technology (HCMUT), VNU-HCM, for supporting this study. The authors express their gratitude to the AVL Company in Austria for supplying the AVL BOOST software.

## REFERENCES

[1] Chen, Y. et al.: A comprehensive review of stability enhancement strategies for metal nanoparticle additions to diesel/biodiesel and their methods of reducing pollutant, Process Saf. Environ. Prot., Vol. 183, p. 1258–1282, 2024.

[2] Nestorović, D., Jovanović, V.V., Manić, N.G., Stojiljković, D.D.: Engine and road tests of blends of biodiesel and diesel fuel, FME Trans., Vol. 40, No. 3, pp. 127–133, 2012.

[3] Deng, S., Mi, Z.: A review on carbon emissions of global shipping, Mar. Dev., Vol. 1, p. 4, 2023.

[4] Ranjit, P.S., Bhurat, S.S., Thakur, A.K., Mahesh, G.S., Reddy, M.S.: Experimental investigations on hydrogen supplemented Pinus Sylvestris oil-based diesel engine for performance enhancement and reduction in emissions, FME Trans., Vol. 50, No. 2, pp. 313–321, 2022.

[5] Yüksek, L., Kaleli, H., Özener, O., Özoğuz, B.: The effect and comparison of biodiesel-diesel fuel on crankcase oil, diesel engine performance and emissions, FME Trans., Vol. 37, No. 2, pp. 91–97, 2009.

[6] Loulergue, L., Schilt, A., Spahni, R., et al.: Orbital and millennial-scale features of atmospheric CH□ over the past 800,000 years, Nature, Vol. 453, pp. 383–386, 2008.

[7] Tock, L. et al.: Thermo-environomic evaluation of the ammonia production, Can. J. Chem. Eng., Vol. 93, No. 2, pp. 356–362, 2015.

[8] Kurien, C., Mittal, M.: Review on the production and utilization of green ammonia as an alternate

fuel in dual-fuel compression ignition engines, En–ergy Convers. Manag., Vol. 251, p. 114990, 2022.

[9] Teoh, Y.H., How, H.G., Le, T.D., Nguyen, H.T., et al.: A review on production and implementation of hydrogen as a green fuel in internal combustion engines, Fuel, Vol. 333, No. Part 2, p. 126525, 2023.

[10] Chiong, M.C., Chong, C.T., Ng, J.H., Mashruk, S., et al.: Advancements of combustion technologies in the ammonia-fuelled engines, Energy Convers. Manag., Vol. 244, p. 114460, 2021.

[11] Cardoso, J.S., Silva, V., Rocha, R.C., Hall, M.J., Costa, M., Eusébio, D.: Ammonia as an energy vector: Current and future prospects for low-carbon fuel applications in internal combustion engines, J. Clean. Prod., Vol. 296, p. 126562, 2021.

[12] Singh, S., Jain, S., PS, V., Tiwari, A.K., Nouni, M.R., Pandey, J.K., et al.: Hydrogen: A sustainable fuel for future of the transport sector, Renew. Sustain. Energy Rev., Vol. 51, pp. 623–633, 20

[13] Ichimura, R., Hadi, K., Hashimoto, N., Hayakawa, A., Kobayashi, H., Fujita, O.: Extinction limits of an ammonia/air flame propagating in a turbulent field, Fuel, Vol. 246, pp. 178–186, 2019.

[14] Xia, Y. et al.: Turbulent burning velocity of ammo–nia/oxygen/nitrogen premixed flame in $O_2$-enriched air condition, Fuel, Vol. 268, p. 117383, 2020.

[15] Xiao, H., Lai, S., Valera-Medina, A., Li, J., Liu, J., Fu, H.: Study on counterflow premixed flames using high concentration ammonia mixed with methane, Fuel, Vol. 275, p. 117902, 2020.

[16] Rocha, R.C., Costa, M., Bai, X.S.: Chemical kinetic modelling of ammonia/hydrogen/air ignition, pre–mixed flame propagation and NO emission, Fuel, Vol. 246, pp. 24–33, 2019.

[17] Feng, Y., Zhu, J., Mao, Y., Raza, M., Qian, Y., Yu, L., et al.: Low-temperature auto-ignition charac–teristics of $NH_3$/diesel binary fuel: Ignition delay time measurement and kinetic analysis, Fuel, Vol. 281, p. 118761, 2020.

[18] Hayakawa, A., Goto, T., Mimoto, R., Arakawa, Y., Kudo, T., Kobayashi, H.: Laminar burning velocity and Markstein length of ammonia/air premixed fla–mes at various pressures, Fuel, Vol. 159, pp. 98–106, 2015.

[19] Nayak-Luke, R., Bañares-Alcántara, R., Wilkinson, I.: "Green" Ammonia: Impact of Renewable Ener–gy Intermittency on Plant Sizing and Levelized Cost of Ammonia, Ind. Eng. Chem. Res., Vol. 57, No. 43, pp. 14698–14708, 2018.

[20] Siddiqui, O., Dincer, I.: A new solar energy system for ammonia production and utilization in fuel cells, Energy Convers. Manag., Vol. 208, p. 112590, 2020.

[21] Reiter, A.J., Kong, S.C.: Demonstration of compre–ssion-ignition engine combustion using ammonia in reducing greenhouse gas emissions, Energy Fuels, Vol. 22, pp. 2963–2971, 2008.

[22] Pei, Y., Wang, D., Jin, S., Gu, Y., Wu, C., Wu, B.: A quantitative study on the combustion and emission characteristics of an ammonia-diesel dual-fuel (ADDF) engine, Fuel Process. Technol., Vol. 250, p. 107906, 2023.

[23] Mi, S., Wu, H., Pei, X., Liu, C., Zheng, L., Zhao, W., et al.: Potential of ammonia energy fraction and diesel pilot-injection strategy on improving combustion and emission performance in an ammonia-diesel dual fuel engine, Fuel, Vol. 343, p. 127889, 2023.

[24] Xu, L., Xu, S., Bai, X.S., Repo, J.A., Hautala, S., Hyvönen, J.: Performance and emission charac–teristics of an ammonia/diesel dual-fuel marine engine, Renew. Sustain. Energy Rev., Vol. 185, p. 113631, 2023.

[25] Yousefi, A., Guo, H., Dev, S., Liko, B., Lafrance, S.: Effects of ammonia energy fraction and diesel injection timing on combustion and emissions of an ammonia/diesel dual-fuel engine, Fuel, Vol. 314, p. 122723, 2022.

[26] Liu, L., Wu, J., Liu, H., Wu, Y., Wang, Y.: Study on marine engine combustion and emissions chara–cteristics under multi-parameter coupling of ammo–nia-diesel stratified injection mode, Int. J. Hydro–gen Energy, Vol. 48, No. 26, pp. 9881–9894, 2023.

[27] Shin, J., Park, S.: Numerical analysis and optimi–zation of combustion and emissions in an ammonia-diesel dual-fuel engine using an ammonia direct injection strategy, Energy, Vol. 289, p. 130014, 2024.

[28] Ryu, K., Zacharakis-Jutz, G.E., Kong, S.C.: Perfor–mance enhancement of ammonia-fueled engine by using dissociation catalyst for hydrogen generation, Int. J. Hydrogen Energy, Vol. 39, No. 5, pp. 2390–2398, 2014.

[29] Castresana, J., Gabiña, G., Martín, L., Uriondo, Z.: Comparative performance and emissions assess–ments of a single-cylinder diesel engine using arti–ficial neural network and thermodynamic simula–tion, Appl. Therm. Eng., Vol. 185, p. 116343, 2021.

[30] Rubio, J.A.P., Vera-García, F., Grau, J.H., Cámara, J.M., Hernandez, D.A.: Marine diesel engine failure simulator based on thermodynamic model, Appl. Therm. Eng., Vol. 144, pp. 982–995, 2018.

[31] Aldhaidhawi, M., Chiriac, R., Bădescu, V., Descombes, G., Podevin, P.: Investigation on the mixture formation, combustion characteristics and performance of a diesel engine fueled with diesel, biodiesel B20 and hydrogen addition, Int. J. Hydrogen Energy, Vol. 42, No. 26, pp. 16793–16807, 2017.

[32] Rimkus, A., Berioza, M., Melaika, M., Juknelevičius, R., Bogdanovičius, Z.: Improvement of the compression-ignition engine indicators using dual fuel (diesel and liquefied petroleum gas), Procedia Eng., Vol. 134, pp. 30–39, 2016.

[33] Lasocki, J., Bednarski, M., Sikora, M.: Simulation of ammonia combustion in dual-fuel compression-

ignition engine, IOP Conf. Ser.: Earth Environ. Sci., Vol. 214, No. 1, p. 012081, 2019.

[34] Hong, T.D., Nguyen, B.N., Truong, P.T., Do, S.H., et al.: Application of AVL BOOST modeling to optimize the engine working load and drivetrain transmission ratio of the diesel firefighting pump system, Heliyon, Vol. 10, No. 24, p. e41029, 2024.

[35] Hong, T.D., Nguyen, B.N., Pham, M.Q., Vu, T.V., Do, S.H.: A comparative investigation of the operating performance and emission characteristics of various diesel engines driving the firefighting pump, Results Eng., Vol. 22, p. 102243, 2024.

[36] Li, T., Zhou, X., Wang, N., Wang, X., Chen, R., Li, S., et al.: A comparison between low- and high-pressure injection dual-fuel modes of diesel-pilot-ignition ammonia combustion engines, J. Energy Inst., Vol. 102, pp. 362–373, 2022.

[37] Niki, Y.: Experimental and numerical analysis of unburned ammonia and nitrous oxide emission characteristics in ammonia/diesel dual-fuel engine, Int. J. Engine Res., Vol. 24, No. 9, pp. 4190–4203, 2023.

[38] ISO 8528-1:2018: Reciprocating internal combus–tion engine driven alternating current generating sets — Part 1: Application, ratings and perfor–mance, International Organization for Standardi–zation, 2018.

[39] Hong, T.D., Xuan, H., Hung, T., Hoang, S., et al.: Effect of ignition timing and combustion duration on the performance characteristics of a diesel engine using vibe 2-zone model, FME Trans., Vol. 52, No. 4, pp. 544–555, 2024.

[40] RV50 Vikyno diesel engines RV125-2, RV145-2LX, in Vikyno Diesel Engine Specifications, Edges Rural Supplies, 2014.

[41] AVL: User Guide AVL Boost, AVL LIST GmbH, 2022.

[42] Hu, Z., Yin, Z., An, Y., Pei, Y.: Ammonia as fuel for future diesel engines, in Diesel Engines - Current Challenges and Future Perspectives, H. Koteen (Ed.), IntechOpen, 2023.

[43] Jamrozik, A., Tutak, W.: The impact of ammonia and hydrogen additives on the combustion characteristics, performance, stability and emissions of an industrial DF diesel engine, Appl. Therm. Eng., Vol. 257, No. Part A, p. 124189, 2024.

[44] Nguyen, V.T., Do, S.H., Pham, M.Q., Wang, W.C., Hong, T.D.: Optimal ignition timing prediction based on premixed ratio and combustion duration using the multiple Vibe 2-Zone combustion model, J. Eng., 2025.

[45] Yu, W., Zhang, Z., Liu, B.: Investigation on the performance enhancement and emission reduction of a biodiesel fueled diesel engine based on an improved entire diesel engine simulation model, Processes, Vol. 9, No. 1, p. 104, 2021.

[46] Duong, L.H., Do, S.H., Vo, H.X., Pham, M.Q., Vu, T.V., Hong, T.D.: Comparative study of Vibe 2-Zone and Multiple Vibe 2-Zone combustion models on combustion, performance, and emissions of a diesel engine, Transp. Eng., Vol. 20, p. 100348, 2025.

[47] Nguyen, V.T., Tran, K.T., Luong, T.H., Pham, M.Q., Wang, W.C., Hong, T.D.: Simulation and analysis of performance, combustion, and emissions of a stationary diesel engine fueled with diesel-LPG blends, Results Eng., Vol. 28, p. 108221, 2025.

[48] Hong, T.D., Hoang, B.T.T., Ho, T.Q.M., Pham, M.Q.: An experimental investigation on the performance of a single cylinder diesel engine at various partial loads, Transp. Eng., Vol. 18, p. 100288, 2024.

[49] Nadimi, E., Przybyła, G., Lewandowski, M.T., Adamczyk, W.: Effects of ammonia on combustion, emissions, and performance of the ammonia/diesel dual-fuel compression ignition engine, J. Energy Inst., Vol. 107, p. 101158, 2023.

[50] Shayler, P.J., Leong, D.K.W., Murphy, M.W.: Contributions to engine friction during cold, low speed running and the dependence on oil viscosity, SAE Tech. Pap., 2005.

[51] Shayler, P.J., Leong, D.K.W., Murphy, M.W.: Friction teardown data from motored engine tests on light duty automotive diesel engines at low temperatures and speeds, in Proc. ASME 2003 Int. Combust. Eng. Rail Transp. Div. Fall Tech. Conf., 2003.

[52] AVL: Theory AVL Boost, AVL LIST GmbH, 2022.

[53] Hong, C., Ji, C., Wang, S., Xin, G., Qiang, Y., Yang, J.: Evaluation of hydrogen injection and oxygen enrichment strategies in an ammonia-hydrogen dual-fuel engine under high compression ratio, Fuel, Vol. 354, p. 129244, 2023.

[54] Fernández-Tarrazo, E., Gómez-Miguel, R., Sánchez-Sanz, M.: Minimum ignition energy of hydrogen–ammonia blends in air, Fuel, Vol. 337, p. 127128, 2023.

[55] Tornatore, C., Marchitto, L., Sabia, P., De Joannon, M.: Ammonia as green fuel in internal combustion engines: State-of-the-art and future perspectives, Front. Mech. Eng., Vol. 8, p. 944201, 2022.

[56] Gross, C.W., Kong, S.C.: Performance characte–ristics of a compression-ignition engine using direct -injection ammonia–DME mixtures, Fuel, Vol. 103, pp. 1069–1079, 2013.

[57] Imtenan, S., Masjuki, H.H., Varman, M., Fattah, I.M.R., Sajjad, H., Arbab, M.I.: Effect of n-butanol and diethyl ether as oxygenated additives on com–bustion–emission–performance characteristics of a multiple cylinder diesel engine fuelled with diesel–jatropha biodiesel blend, Energy Convers. Manag., Vol. 94, pp. 84–94, 2015.

[58] Xiao, H., Guo, F., Li, S., Wang, R., Yang, X.: Combustion performance and emission characte–ristics of a diesel engine burning biodiesel blended with n-butanol, Fuel, Vol. 258, p. 115887, 2019.

[59] Mathieu, O., Petersen, E.L.: Experimental and modeling study on the high-temperature oxidation

of ammonia and related NOx chemistry, Combust. Flame, Vol. 162, No. 3, pp. 554–570, 2015.

[60] Liu, J.H., Liu, J.L.: Experimental investigation of the effect of ammonia substitution ratio on an ammonia-diesel dual-fuel engine performance, J. Clean. Prod., Vol. 434, p. 140274, 2024.

## NOMENCLATURE

| | |
|---|---|
| $A$ | surface area |
| $C$ | gas velocity coefficient/ model constant |
| $h$ | enthalpy |
| $m$ | mass |
| $p$ | pressure |
| $P$ | power |
| $Q$ | energy/ heat loss |
| $T$ | temperature |
| $V$ | volume |

### *Greek symbols*

| | |
|---|---|
| $\alpha$ | crankshaft angle |
| $\alpha_w$ | heat transfer effectiveness |

### *Subscripts*

| | |
|---|---|
| b | burned |
| c | cylinder |
| c,0 | motorized condition |
| c,1 | intake valve closing (IVC) |
| F | fuel |
| i | instantaneous/ surface index |
| sim | simulation |
| u | unburned |
| w | wall |
| D | displacement |

## APPENDIX A. COMBUSTION CHARACTERISTICS OF THE ENGINE AT 900RPM

### A.1 Influence of diesel-ammonia blend proportions on in-cylinder pressure and heat release rate

Figure A1. shows the in-cylinder pressure profiles for combustion using pure diesel as the reference case and for the co-combustion of diesel with ammonia at an engine speed of 900. At the CD80 operating point, the peak of HRR is higher than that of the reference diesel fuel at both 900 rpm. At 900 rpm, the peak of HRR increases from 39.58 J/deg (0RAE) to 40.27 J/deg (10RAE).

In addition, this peak is progressively delayed as the ammonia content increases. Relative to the 0RAE baseline, this delay reaches 0.7°, 0.9°, 1.2°, 1.4°, and 1.6° crank angle (CA) for the 2RAE to 10RAE blends, respectively.

The higher total heat released during this concentrated combustion phase results in an elevated peak of in-cylinder pressures compared to the 0RAE baseline. The peaks of pressures for the 2RAE and 4RAE blends rise slightly to 58.65 bar and 58.67 bar, respectively, whereas the pressure peaks for the 6RAE, 8RAE, and 10RAE blends show very slight decreases to 58.56 bar, 58.60 bar, and 58.63 bar, respectively.

At CD100, the crank angle corresponding to the maximum HRR increases from 0.8° to 2.8° for the 10RAE blend, while the peak value of HRR remains essentially unchanged.

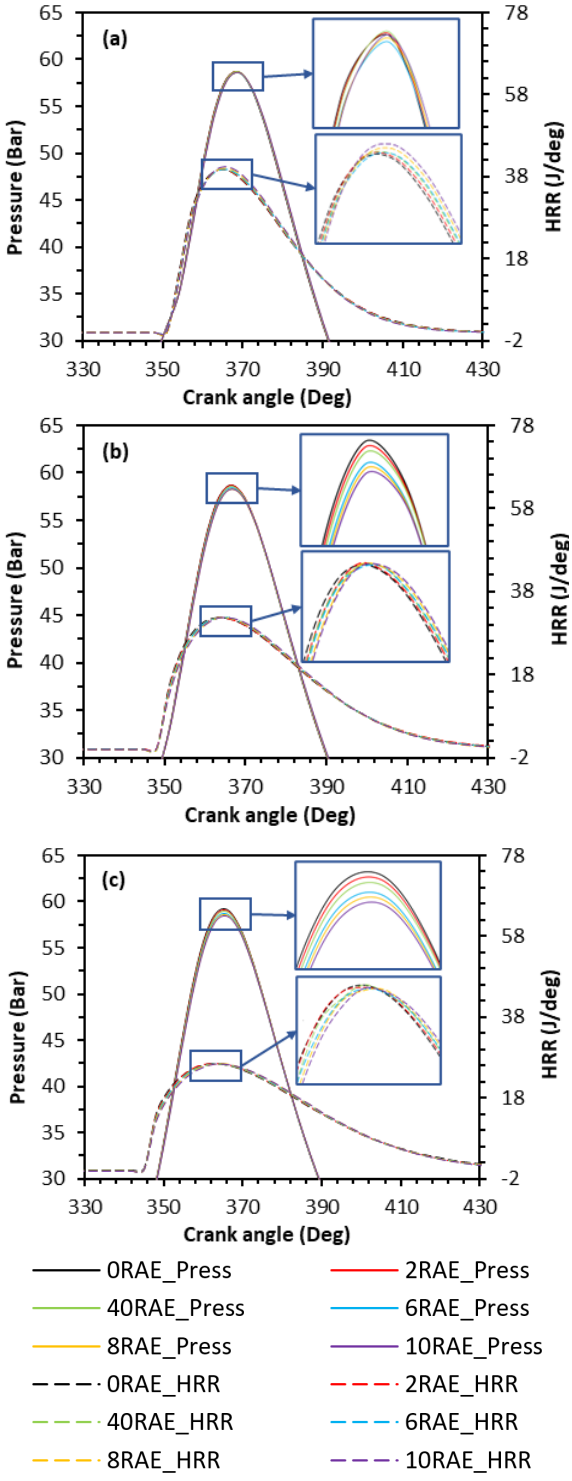


**Figure A1. In-cylinder pressure and heat release rate at 85% load for ammonia–diesel blends at 900rpm: (a) CD80, (b) CD100, (c) CD120.**

Concurrently, the peak in-cylinder pressure decreases by 0.09, 0.17, 0.35, 0.42, and 0.50 bar for the 2RAE through 10RAE blends, respectively. At CD120, both a slight reduction in the magnitude and a retardation in the timing of the heat release rate are observed. Cylinder pressure also declines with increasing ammonia content: at 900 rpm, the reductions amount to 0.12, 0.23, 0.46, 0.56, and 0.67 bar for the 2RAE to 10RAE blends, respectively.

### A.2 Influence of diesel-ammonia blend proportions on temperature

Figure A2 shows the in-cylinder temperature variations for various diesel–ammonia blend ratios at three com–bustion phases (CD80, CD100, and CD120) under 85% load and 900 rpm.

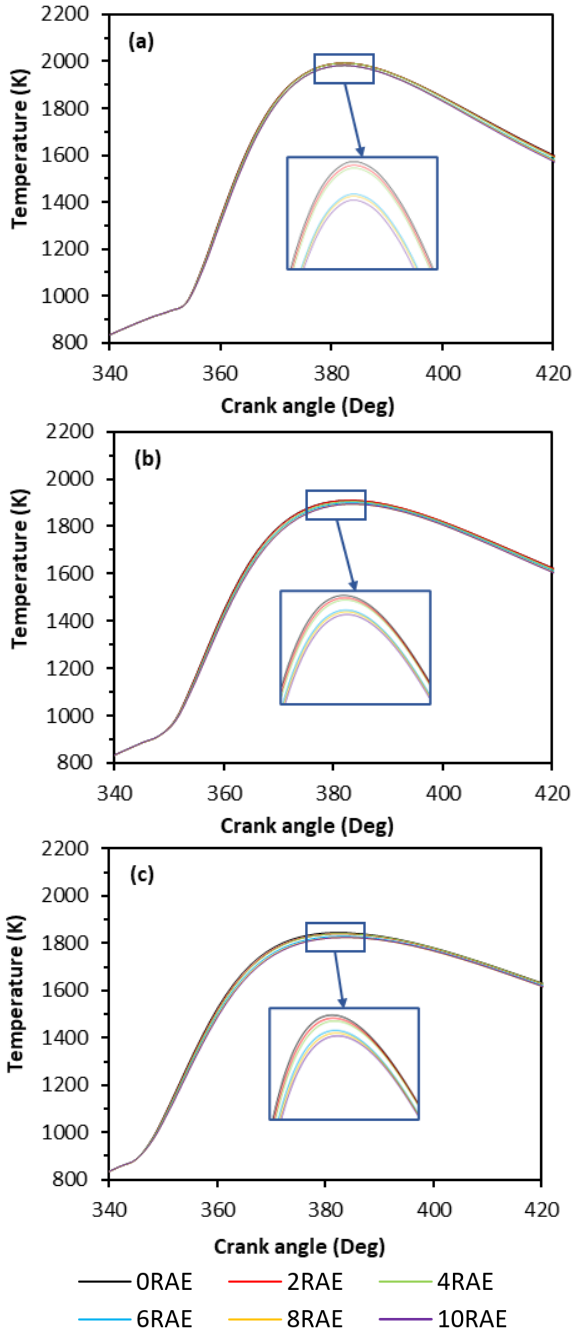


**Figure A2. In-cylinder temperature at 85% load for ammonia–diesel blends at 900rpm: (a) CD80, (b) CD100, (c) CD120.**

The temperature trends with increasing $NH_3$ substi–tution ratio closely resemble those observed at 2400 rpm. Specifically, the peak of in-cylinder temperature decreases by 0.74%, 0.90%, and 1.10% at CD80, CD100, and CD120, respectively.

## НУМЕРИЧКА АНАЛИЗА ПЕРФОРМАНСИ, САГОРЕВАЊА И ЕМИСИЈА СТАЦИОНАРНОГ ДИЗЕЛ МОТОРА КОЈИ РАДИ НА МЕШАВИНЕ АМОНИЈАКА И ДИЗЕЛА

**М.Х. Ха, Б.Т. Тран, Н.К. Ле, М.К. Фан, К.Т.Ф. Нгием, Т.Д. Хонг**

Амонијак привлачи пажњу као перспективно алтер–нативно гориво због свог састава без угљеника и потенцијала за смањење штетних емисија. Ова сту–дија истражује утицај амонијака, који се користи као двоструко гориво са дизелом при концентрацији енергије амонијака од 10% или мање, на сагоревање, перформансе и емисије стационарног једноцилин–дричног мотора са компресионим паљењем, корис–тећи AVL BOOST симулациони модел. Мотор RV-125, популаран модел за рурална подручја у Вијет–наму, пројектован је да ради у опсегу брзина од 900 до 2400 о/мин при оптерећењу мотора од 85%, са три различита трајања сагоревања: 80, 100 и 120 степени угла радилице (CD80, CD100 и CD120). Резултати показују да повећање садржаја амонијака на 10% енергије горива незнатно побољшава снагу мотора за приближно 1%, али такође доводи до веће потрошње горива специфичне за кочење због ниже густине енергије амонијака. Када је амонијак при–сутан у смеши, врхови брзине ослобађања топлоте (HRR) и притиска у цилиндру се благо повећавају на CD80, али се благо смањују на CD100 и CD120; у међувремену, утврђено је да врх температуре у цилиндру постепено опада са дужим вредностима CD, а времена врхова HRR, притиска у цилиндру и температуре су благо успорена. Резултати такође показују да мешање амонијака значајно смањује емисије NOx за више од 22% и емисије CO за приближно 27%, док емисије чађи остају практично непромењене. Студија закључује да мешање амони–јака представља обећавајућу алтернативу за ублажа–вање штетних загађивача и емисија гасова стаклене баште без угрожавања снаге или ефикасности мо–тора. Овај рад пружа кључну основу за будућа ист–раживања усмерена на примену амонијачног горива за рурални развој у Вијетнаму.